

Metal–Insulator Transitions in the Falicov–Kimball Model with Disorder

Krzysztof Byczuk

Institute of Theoretical Physics, Warsaw University, ul. Hoża 69, PL-00-681 Warszawa, Poland

(Dated: July 14, 2018)

The ground state phase diagrams of the Falicov–Kimball model with local disorder is derived within the dynamical mean–field theory and using the geometrically averaged (“typical”) local density of states. Correlated metal, Mott insulator and Anderson insulator phases are identified. The metal–insulator transitions are found to be continuous. The interaction and disorder compete with each other stabilizing the metallic phase against occurring one of the insulators. The Mott and Anderson insulators are found to be continuously connected.

PACS numbers: 71.10.Fd, 71.27.+a, 71.30.+h, 72.80.Ng

I. INTRODUCTION

Motion of quantum particles can be suppressed or even destroyed by Coulomb interactions and disorder, which are the driving forces behind a metal–insulator transition (MIT). The Mott–Hubbard MIT is caused by Coulomb correlations in the pure system, i.e. without disorder.¹ The Anderson MIT, also referred to the Anderson localization, is due to coherent backscattering from randomly distributed impurities in a system without interaction.² The properties of real materials are strongly influenced by both interaction and randomness.³ It is therefore a challenge to investigate quantum models where both correlations and disorder are simultaneously present.^{4,5,6,7}

The Mott–Hubbard MIT is characterized by opening a gap in the density of states at the Fermi level.⁸ At the Anderson localization the character of the spectrum at the Fermi level changes from continuous one to dense pure point one.⁹ It is plausible that both MITs could be detected by knowing a single quantity, namely, a local density of states (LDOS). Although the LDOS is not an order parameter associated with a symmetry breaking phase transition,⁵ it discriminates between a metal and an insulator, which is driven by correlations and disorder.

In a disordered system the LDOS depends on particular realization of the disorder. Then the entire probability distribution function of the LDOS is required to know,¹⁰ which is a very demanding task. Instead one could use certain moments of the LDOS. This however is insufficient because the arithmetically averaged LDOS (first moment) stays finite at the Anderson MIT.¹¹ It was already pointed out by Anderson² that the “typical” values of random quantities, which are mathematically given by the most probable values of the probability distribution functions,¹² should be used to describe localization. The *geometric* mean^{13,14} gives an approximation of the most probable (“typical”) value of the LDOS and vanishes at a critical strength of the disorder, hence providing an explicit criterion for Anderson localization.^{2,15,16,17}

Theoretical descriptions of the MIT has to be non–perturbative if no long–range order exists on either side of the transition. In such a case there is no obvious order parameter and no Landau type functional available. A non–perturbative framework for investigation of the

Mott–Hubbard MIT in lattice electrons with a local interaction and disorder is given by dynamical mean–field theory (DMFT).^{18,19,20,21} If in this approach the effect of local disorder is taken into account through the arithmetic mean of the LDOS²² one obtains, in the absence of interactions, the well known coherent potential approximation (CPA),²³ which does not describe the physics of Anderson localization. To overcome this deficiency Dobrosavljević and Kotliar¹⁵ formulated a variant of the DMFT where the geometrically averaged LDOS is computed from the solutions of the self–consistent stochastic DMFT equations. Subsequently, Dobrosavljević *et al.*¹⁶ incorporated the geometrically averaged LDOS into the self–consistency cycle and thereby derived a mean–field theory of Anderson localization which reproduces many of the expected features of the disorder–driven MIT for non–interacting electrons. This scheme uses only one–particle quantities and is therefore easily incorporated into the DMFT for disordered electrons in the presence of phonons,²⁴ or Coulomb correlations.⁷ In particular, the non–magnetic ground state phase diagram of the Anderson–Hubbard model at half–filling was derived.⁷

In this paper we investigate the Falicov–Kimball model²⁵ with a local disorder. The pure Falicov–Kimball model describes two species of particles, mobile and immobile, which interact with each other when both are on the same lattice site.^{25,26} The Falicov–Kimball model captures some aspects of the Mott–Hubbard MIT, i.e. upon increasing the interaction the LDOS for mobile particles splits into two subbands opening a correlation gap at the Fermi level if $n_e + n_f = 1$, where n_e (n_f) is the density of mobile (immobile) particles.^{26,27,28,29} Here we introduce the *Anderson–Falicov–Kimball model* where the mobile particles are disturbed by a local random potential. Our aim is to obtain a phase diagram of such a model and to identify MITs driven by correlations and disorder. We find a subtle competition between interaction and disorder yielding stabilization of metallicity in the Anderson–Falicov–Kimball model. The model is solved within the DMFT framework combined with geometric averaging of the LDOS. The results are compared with those obtained within the DMFT with arithmetic averages. Only geometric averaging yields the Anderson transition.

In Section II we define the Anderson–Falicov–Kimball model and present the DMFT equations which provide the solution of this model. In Section III and IV numerical results concerning the ground state phase diagram are shown and discussed in details. The analytical approach to the MIT in the band center is developed in Section V. Section VI presents our conclusions and final remarks.

II. ANDERSON–FALICOV–KIMBALL MODEL

A. The Model

The Anderson–Falicov–Kimball model is defined by the following Hamiltonian

$$H = \sum_{ij} t_{ij} c_i^\dagger c_j + \sum_i \epsilon_i c_i^\dagger c_i + U \sum_i f_i^\dagger f_i c_i^\dagger c_i, \quad (1)$$

where c_i^\dagger (f_i^\dagger) and c_i (f_i) are fermionic creation and annihilation operators for *mobile* (*immobile*) particles at a lattice site i . t_{ij} is a hopping amplitude for mobile particles between sites i and j , and U is the local interaction energy between mobile and immobile particles occupying the same site. The ionic energy ϵ_i is a random, independent variable in our problem, describing the local disorder disturbing a motion of mobile particles. We have assumed that only mobile particles are subjected to the structural disorder. This assumption could be relaxed in further generalizations of the model.

The position of the immobile particles on a lattice is random if there is no long-range order. Therefore, we assume that the occupation number $f_i^\dagger f_i$ on the i -th site is equal to one with probability w ($0 \leq w \leq 1$) and zero with probability $1 - w$. The presence of the randomly distributed immobile particles introduces additional disorder apart of that given by the ϵ_i -term in the Hamiltonian (1). However, the U -term in the Hamiltonian (1) must be treated differently from the ϵ_i -term. The U -term is operator valued in the immobile particle Fock subspace and one has to take the quantum mechanical average over a given quantum state of the f -particles. In contrast, the ϵ_i -term does not depend on the f operators and one has to average the quantum mechanical expectation values over different realizations of ϵ_i or one has to study the whole statistics of an interesting quantum mechanical expectation value. Whereas, the U -term does not change the extended states into the localized ones, the ϵ_i -term can lead to such a change and thereby to the Anderson localization.

In this paper we use the canonical description, where the number of the immobile and mobile particles are independent of each other and fixed. In the pure Falicov–Kimball model increasing the interaction leads to opening a correlation (Mott) gap in the spectrum at $U = U_c$.^{26,27,28,29} If $n_e + n_f = 1$ the Fermi energy for mobile particles is inside of this correlation gap, which means that the ground state is incompressible. On the

Bethe lattice with the band-width W the critical interaction obtained within the DMFT is $U_c = W/2$ for $n_e = n_f = 1/2$.^{26,27,28,29} How the disorder changes this gap and how the localized states enter into the mobile particle band are the subjects of the present study. We neglect any long-range order, which might be achieved on a fully frustrated lattice.¹⁹

B. Dynamical Mean-Field Theory

The Anderson–Falicov–Kimball model, where the interaction and disorder are local, is solved within the DMFT.^{19,20,21,30} Introducing a single and double-particle (Zubarev) Green functions³¹ $G_{ij}(\omega) = \langle\langle c_i | c_j^\dagger \rangle\rangle_\omega$ and $\Gamma_{ij}(\omega) = \langle\langle f_i^\dagger f_i c_i | c_j^\dagger \rangle\rangle_\omega$, respectively, we derive the equations of motion

$$(\omega + \mu - \epsilon_k) G_{kl}(\omega) - \sum_j t_{kj} G_{jl}(\omega) = \delta_{kl} + U \Gamma_{kl}(\omega), \quad (2a)$$

$$(\omega + \mu - \epsilon_k - U) \Gamma_{kl}(\omega) = \langle f_k^\dagger f_k \rangle \delta_{kl} + \sum_j t_{kj} \Gamma_{jl}(\omega), \quad (2b)$$

where we used that a number of the immobile particles is conserved being zero or one, and hence $f_i^\dagger f_i f_i^\dagger f_i = f_i^\dagger f_i$. The chemical potential μ is introduced only for the mobile subsystem and ω denotes the energy. Defining the site-independent self-energy, according to DMFT scheme,^{30,32}

$$\Sigma(\omega, \epsilon_i) \equiv U \frac{\Gamma_{ij}(\omega)}{G_{ij}(\omega)}, \quad (3)$$

which depends implicitly on ϵ_i , the system of the equations (2) can be solved yielding an explicit formula for the self-energy

$$\Sigma(\omega, \epsilon_i) = wU + \frac{w(1-w)U^2}{\omega + \mu - \epsilon_i - (1-w)U - \eta(\omega)}. \quad (4)$$

We defined the averaged number of localized particles per site $\langle f_i^\dagger f_i \rangle = n_f = w$ and we introduced the hybridization function $\eta(\omega)$ which is a *dynamical mean field* (*molecular field*) describing the coupling of a selected lattice site with a rest of the system. The local non-interacting Green function is $G_{ii}^0(\omega) = 1/[\omega + \mu - \epsilon_i - \eta(\omega)] \equiv G^0(\omega, \epsilon_i)$.

Using the self-energy $\Sigma(\omega, \epsilon_i)$ and the hybridization function $\eta(\omega)$ we obtain a local (ϵ_i -dependent) Green function

$$G_{ii}(\omega) = \frac{1}{\omega + \mu - \epsilon_i - \eta(\omega) - \Sigma(\omega, \epsilon_i)} \equiv G(\omega, \epsilon_i), \quad (5)$$

and hence the ϵ_i -dependent LDOS

$$A(\omega, \epsilon_i) = -\frac{1}{\pi} \text{Im} G(\omega, \epsilon_i). \quad (6)$$

From the ϵ_i -dependent LDOS (6) we obtain either the geometrically averaged LDOS

$$A_{\text{geom}}(\omega) = \exp[\langle \ln A(\omega, \epsilon_i) \rangle_{\text{dis}}] \quad (7)$$

or the arithmetically averaged LDOS

$$A_{\text{arith}}(\omega) = \langle A(\omega, \epsilon_i) \rangle_{\text{dis}}, \quad (8)$$

where $\langle O(\epsilon_i) \rangle_{\text{dis}} = \int d\epsilon_i \mathcal{P}(\epsilon_i) O(\epsilon_i)$ is an arithmetic mean of $O(\epsilon_i)$.³³ Here we used that ϵ_i are independent random variables characterized by a probability distribution function $\mathcal{P}(\epsilon_i)$. The lattice, i.e. translationally invariant, Green function is given by the corresponding Hilbert transform

$$G(\omega) = \int d\omega' \frac{A_\alpha(\omega')}{\omega - \omega'}, \quad (9)$$

where the subscript α stands for either "geom" or "arith". The Dyson self-energy $\Sigma(\omega)$ is determined from the \mathbf{k} -integrated Dyson equation $\Sigma(\omega) = \omega - \eta(\omega) - 1/G(\omega)$. The self-consistent DMFT equations are closed through the Hilbert transform $G(\omega) = \int d\epsilon N_0(\epsilon) / [\omega - \epsilon - \Sigma(\omega)]$, which relates the lattice Green function to the self-energy; here $N_0(\epsilon)$ is the non-interacting density of states.

The DMFT which uses A_{arith} is an exact approach in the limit of infinite dimension where quantum mechanical rescaling is imposed on hopping amplitudes.^{18,23} On the other hand, the mathematically rigorous limit for the DMFT with A_{geom} is not yet known.¹⁶ Nevertheless, it is very promising single site theory which has the ability to describe at least some aspect of the Anderson localization, i.e. the localization due to random fluctuations of the wave function amplitude.³⁴ As a single site theory, it cannot capture interference effects due to fluctuations of a phase of the wave function and, thereby, weak localization aspects are not recovered.

The Anderson-Falicov-Kimball model (1) is solved for a semi-elliptic density of states for the Bethe lattice, $N_0(\epsilon) = 4\sqrt{1 - 4(\epsilon/W)^2}/(\pi W)$. Then $\eta(\omega) = W^2 G(\omega)/16$. For a probability distribution function $\mathcal{P}(\epsilon_i)$ we assume a box model, i.e. $\mathcal{P}(\epsilon_i) = \Theta(\Delta/2 - |\epsilon_i|)/\Delta$, with Θ as the step function. The parameter Δ is a measure of the disorder strength. For numerical integrations we use discrete values of ϵ_i selected according to the Gauss-Legendre algorithm. The number of ϵ_i levels depends on Δ and is adjusted such to obtain smooth density of states. The chemical potential $\mu = U/2$, corresponding to half-filled conducting band (i.e., $n_e = 1/2$), and $w = 1/2$ are assumed in this paper. $W = 1$ sets the energy units.

C. Criteria for Anderson and Mott MIT

The arithmetically averaged LDOS $A_{\text{arith}}(\omega)$ at the energy ω in a band is always positive for non-interacting systems with disorder.¹¹ This quantity is non-critical for

the Anderson localization. However it approaches zero when the gap is opened at energy ω in the spectrum of the correlated system. On the other hand $A_{\text{geom}}(\omega)$ vanishes at the Anderson localization. We therefore classify the states at energy ω as localized by disorder if $A_{\text{geom}}(\omega) = 0$ and $A_{\text{arith}}(\omega) > 0$. When both $A_{\text{geom}}(\omega) = 0$ and $A_{\text{arith}}(\omega) = 0$ it means that the states at energy ω are absent due to correlations.

III. SPECTRAL PHASE DIAGRAMS

Depending on the spectral properties of the Anderson-Falicov-Kimball model we distinguish three different regimes: i) weak interaction regime for $0 < U < W/2$, ii) intermediate interaction regime for $W/2 < U \lesssim 1.36W$, and iii) strong interaction regime for $U \gtrsim 1.36W$. Examples of the spectral phase diagrams on the energy-disorder ($\omega - \Delta$) planes in these three regimes are shown in Fig. 1 in the upper, middle, and lower panels, respectively.

In the weak interaction regime (i) the Mott gap is not opened. Increasing the disorder strength Δ leads to narrowing of the spectrum with extended gapless states (continuous spectrum) and to broadening of the total bandwidth. This is illustrated in Fig. 2 presenting the evolution of $A_{\text{geom}}(\omega)$ and $A_{\text{arith}}(\omega)$, upper and lower panels respectively, upon increasing Δ . The continuous spectrum corresponds to a support of $A_{\text{geom}}(\omega)$, i.e. such an energy window for which $A_{\text{geom}}(\omega) > 0$, whereas the full band is given by the support of $A_{\text{arith}}(\omega)$. The trajectories of the band edges (dashed lines) determined within the DMFT with arithmetic averaging and the trajectory of mobility edge (solid lines) determined within the DMFT with geometric averaging are shown in Fig. 1. In the weak interaction regime the localized gapless states (pure point spectrum) are in a compact part of the spectral phase diagram between the mobility and band edges. The spectral phase diagram of the Anderson-Falicov-Kimball model in the weak interaction regime (i) is qualitatively similar to that of the Anderson model without the interaction.¹⁶

In the intermediate interaction regime (ii) the Mott gap is opened at $\Delta = 0$, as is shown in Fig. 3. Upon increasing Δ the Mott gap is shrunk and finally closed, cf. Fig. 3. The disorder redistribute the spectral weight filling in the correlation gap completely by continuous spectrum. The spectral phase diagram is shown in the middle panel of Fig. 1. As previously the total bandwidth, determined by $A_{\text{arith}}(\omega)$, increases by increasing Δ . However in contrast to (i), in the present case there are two trajectories representing external (from the band gap sides) and internal (from the Mott gap sides) mobility edges. Similarly there are two band-edge trajectories, external and internal ones. The extended gapless states are bounded between mobility edge trajectories as is shown in the middle panel of Fig. 1. Two separated regions with localized gapless states are bounded by the

mobility edge and the band edge trajectories. If the correlation gap is opened, the localized states appear in the spectrum from each side of the Hubbard subbands.

In the strong interaction regime (iii) the Mott gap, determined within the DMFT framework with geometrical averaging, is never filled in even at large disorder. The LDOS given by $A_{\text{geom}}(\omega)$ and shown in Fig. 4 always has two separate parts, remnants of the lower and the upper Hubbard subbands. This is in contrast with the DMFT framework with arithmetic averaging where these two subbands always merge if Δ is sufficiently large. It means that the Mott gap is only filled in by localized states when the disorder increases. In the spectral phase diagram the spectrum of extended states is given by two separate lobes bounded by the mobility edge trajectories, as in the lower panel of Fig. 1. At $\Delta > 0$ these lobes are surrounded by localized gapless states.

IV. BAND CENTER

In the half-filled band case the ground state properties are solely determined by the character of quantum states in the band center ($\omega = 0$). Corresponding phase diagrams in the interaction-disorder ($U - \Delta$) plane are shown in Fig. 5 and discussed below. We define three phases: a) *extended gapless phase* (i.e. a gapless phase with extended states at the Fermi level), b) *localized gapless phase* (i.e. a gapless phase with localized states at the Fermi level), and c) *gapped phase* (i.e. a phase with a gap at the Fermi level).

The extended gapless phase (disorder metallic phase), is characterized by a non-zero value of the LDOS. In the pure Falicov-Kimball model the Luttinger theorem is not satisfied and quasiparticles at the Fermi level have finite life-time.³⁵ It means that due to the interaction $A_\alpha(\omega = 0) < N_0(\omega = 0)$ even at $\Delta = 0$. Increasing Δ at fixed U leads to further decreasing of the LDOS as is shown in the upper panel of Fig. 6. Similarly, increasing U at constant Δ leads to decreasing of the LDOS as is presented in the upper panel of Fig. 7.

Mott-Hubbard MIT, represented by $\Delta_c^{MH}(U)$ lines in Fig. 5, occurs at small and intermediate disorder $0 \leq \Delta \lesssim 1.70W$ and the interaction $W/2 \leq U \lesssim 1.36W$. This MIT is continuous one as is seen in the lower panel of Fig. 6 around $\Delta \approx 0.8$ and in Fig. 7 around $U \approx 0.7$ (upper panel) and $U \approx 1.3$ (lower panel). Increasing Δ above $\Delta_c^{MH}(U)$ when $W/2 < U \lesssim 1.36W$ results in a transition from a correlated gapped insulator into a bad metallic phase, as is illustrated in the lower panel of Fig. 6. It means that the disorder stabilizes the metallic phase. Similar Mott-Hubbard MIT is obtained within the DMFT with arithmetic averaging and the corresponding phase diagram is reproduced in the lower panel of Fig. 5.

Anderson MIT line $\Delta_c^A(U)$ is an increasing function of U for $0 \leq U \lesssim 0.95W$ starting from the value $\Delta_c^A = eW/2 \approx 1.36W$ ($e \approx 2.718$ is the Euler constant) in

the non-interacting case.¹⁶ The interaction impedes the localization of particles due to impurity scattering. In particular, for $eW/2 \lesssim \Delta \lesssim 2.03W$ and $0 < U \lesssim 0.95W$ the interaction turns the Anderson insulator into a bad correlated metal, as is shown in the lower panel of Fig. 7.

Mott and Anderson insulators are rigorously defined only for $U > W/2$ with $\Delta = 0$ and only for $\Delta > eW/2$ with $U = 0$, respectively. In the presence of the interaction and disorder this distinction can no longer be made. However, as long as the LDOS shows the characteristic Hubbard subbands (see Fig. 4) one may refer to a *disordered Mott insulator* (gapped phase). With increasing Δ the spectral weight of the Hubbard subbands vanishes and the system becomes a *correlated Anderson insulator* (localized gapless phase). The border between these two types of insulators occurs at $\Delta(U) \approx eW/2\sqrt{2}$ when $U \gg W$. To estimate this value we used the analytical result from Ref. 16. Our estimation is exact when $U \rightarrow \infty$ since the band-width of the Hubbard satellites is rigorously known to be $W/\sqrt{2}$ for the Falicov-Kimball model.³⁶ The results obtained here within DMFT show that the Mott and Anderson insulators are continuously connected. Hence, by changing U and Δ it is possible to move from one type of the insulator to the other without crossing the metallic phase. This is plausible because the Anderson MIT ($U = 0$) and the Mott-Hubbard MIT ($\Delta = 0$) are not associated with a symmetry breaking.

V. LINEARIZED DYNAMICAL MEAN-FIELD THEORY

At the MIT (dots and squares in Fig. 5) the LDOS vanishes in the band center. Therefore, in the vicinity of the MIT but on the metallic side the LDOS is arbitrary small and the transition points on the phase diagram can be determined analytically by linearizing the DMFT equations.^{16,37} In the band center, due to a symmetry of $A_\alpha(\omega)$, we find that $G(0) = -i\pi A_\alpha(0)$ and is purely imaginary. Hence the DMFT self-consistency leads to the following recursive relation $\eta^{(n+1)}(0) = -i\pi W^2 A_\alpha^{(n)}(0)/16$, where the left hand side in the $(n+1)$ -th iteration step is given by the result from (n) -th iteration step. Using Eqs. 5 with 4 and expanding them with respect to small $A_\alpha^{(n)}(0)$ we find from Eq. 6 that

$$A^{(n+1)}(0, \epsilon_i) = \frac{W^2}{16} A_\alpha^{(n)}(0) \Upsilon(\epsilon_i), \quad (10)$$

where

$$\Upsilon(\epsilon) = \frac{\epsilon^2 + (\frac{U}{2})^2}{\left[\epsilon^2 - (\frac{U}{2})^2\right]^2}. \quad (11)$$

The recursive relations within the linearized DMFT (L-DMFT) with geometrical averaging are

$$A_{\text{geom}}^{(n+1)}(0) = A_{\text{geom}}^{(n)}(0) \frac{W^2}{16} \exp \left[\frac{1}{\Delta} \int_{-\Delta/2}^{\Delta/2} d\epsilon \ln \Upsilon(\epsilon) \right], \quad (12)$$

and within L-DMFT with arithmetical averaging are

$$A_{\text{arith}}^{(n+1)}(0) = A_{\text{arith}}^{(n)}(0) \frac{W^2}{16} \left[\frac{1}{\Delta} \int_{-\Delta/2}^{\Delta/2} d\epsilon \Upsilon(\epsilon) \right]. \quad (13)$$

In a metallic phase the recursions are increasing, i.e. $A_{\alpha}^{(n+1)}(0) > A_{\alpha}^{(n)}(0)$, whereas in the insulating phase they are decreasing. Therefore, at the boundary curves between metallic and insulating solutions in Fig. 5 the recursions are constant $A_{\alpha}^{(n+1)}(0) = A_{\alpha}^{(n)}(0)$. This observation leads directly to the exact (within DMFT) equations determining the curves $\Delta = \Delta(U)$, i.e.

$$1 = \frac{W^2}{16} \exp \left[\frac{1}{\Delta} \int_{-\Delta/2}^{\Delta/2} d\epsilon \ln \Upsilon(\epsilon) \right] \equiv \frac{W^2}{16} \exp [I_{\text{geom}}(U, \Delta)], \quad (14)$$

for L-DMFT with geometrical averaging, and

$$1 = \frac{W^2}{16} \left[\frac{1}{\Delta} \int_{-\Delta/2}^{\Delta/2} d\epsilon \Upsilon(\epsilon) \right] \equiv \frac{W^2}{16} I_{\text{arith}}(U, \Delta), \quad (15)$$

for L-DMFT with arithmetical averaging. Both integrals can be evaluated analytically with the results

$$\begin{aligned} I_{\text{geom}}(U, \Delta) = 2 + \\ \ln \left[\left(\frac{U}{2} \right)^2 + \left(\frac{\Delta}{2} \right)^2 \right] - 2 \ln \left[\left(\frac{U}{2} \right)^2 - \left(\frac{\Delta}{2} \right)^2 \right] + \\ \frac{2U}{\Delta} \left[\arctan \left(\frac{\Delta}{U} \right) - \ln \left| \frac{\Delta + U}{\Delta - U} \right| \right], \quad (16) \end{aligned}$$

and

$$I_{\text{arith}}(U, \Delta) = \frac{1}{\left(\frac{U}{2} \right)^2 - \left(\frac{\Delta}{2} \right)^2}. \quad (17)$$

Solutions of Eqs. 14 and 15 are shown as solid curves in the upper and the lower panels of Fig. 5, respectively. We find excellent agreement with the numerical solutions of the full DMFT equations (dots and squares in Fig. 5). At small U the critical disorder strength obtained from (14) increases linearly with the interaction, i.e. $\Delta(U) \approx We/2 + \pi U/2$. This is because the total bandwidth increases linearly with U . At small Δ the solution of Eq. 14 (L-DMFT with geometrical averaging) is found to be $\Delta(U) \approx \sqrt{U^2 - (W/2)^2}$. It turns out that the curve $\Delta(U) = \sqrt{U^2 - (W/2)^2}$ is also an exact solution of Eq. 15 (L-DMFT with arithmetical averaging) for

all $U \geq W/2$. At weak disorder both approaches give the same results.

VI. CONCLUSIONS

In the present paper we introduced the Anderson–Falicov–Kimball model and solved it obtaining the phase diagrams for the ground state with the suppressed long-range order. Three different phases, the disordered metal, the disordered Mott insulator, and the correlated Anderson insulator, were identified. It was shown that correlation and disorder compete with each other stabilizing the metallic phase against occurring one of the insulators. We found that these two insulators are continuously connected.

The phase diagram with the three phases in the ground state for the Anderson–Falicov–Kimball model is similar to the phase diagram for the Anderson–Hubbard model solved within the DMFT with geometric averaging in Ref. 7. There are however important qualitative differences between these two solutions. In the Anderson–Falicov–Kimball model the Mott transition is continuous whereas in the Anderson–Hubbard model there is a hysteresis at low and a crossover transition at high disorder strengths. In addition, in the Anderson–Hubbard model the Luttinger pinning in the disordered metal is reconstructed by strong correlations. This feature is absent in the Anderson–Falicov–Kimball model, where the Luttinger pinning is violated even in the pure case.³⁵

A similar technique, i.e. the DMFT with geometric averaging, could be used to solve other models with disorder and interaction between quantum (mobile) and classical (immobile) degrees of freedom.³⁸ In such cases the self-energy should be given analytically and this removes the problem of using any numerical impurity solver, as was necessary in the Anderson–Hubbard model.⁷ Then not only the LDOS at the Fermi level but also mobility and band edge trajectories can be easily determined. Such models are important for understanding the physics of manganites³⁹ or diluted magnetic semiconductors,^{40,41} where charge carriers are coupled to randomly distributed localized magnetic moments. The role of the disorder and the Anderson localization are inherent for those correlated systems.

Acknowledgments

It is a pleasure to thank R. Lemański for encouraging discussion on this project and critical reading of the manuscript. The author also thanks R. Bulla and D. Vollhardt for useful discussion on different aspects of DMFT and Anderson localization. Financial support through KBN-2 P03B 08 224 is acknowledged. This work was also supported in part by the Sonderforschungsbereich 484 of the Deutsche Forschungsgemeinschaft.

- ¹ N. F. Mott, Proc. Phys. Soc. A **62**, 416 (1949); *Metal-Insulator Transitions*, 2nd edn. (Taylor and Francis, London 1990).
- ² P. W. Anderson, Phys. Rev. **109**, 1492 (1958).
- ³ S. V. Kravchenko, G.V. Kravchenko, J.E. Furneaux, V.M. Pudalov, and M. DiIorio, Phys. Rev. B **50**, 8039 (1994); D. Popović, A. B. Fowler, and S. Washburn, Phys. Rev. Lett. **79**, 1543 (1997); S. V. Kravchenko and M. P. Sarachik, Rep. Prog. Phys. **67**, 1 (2004); H. von Löhneysen, Adv. in Solid State Phys. **40**, 143 (2000).
- ⁴ P. A. Lee and T. V. Ramakrishnan, Rev. Mod. Phys. **57**, 287 (1985).
- ⁵ D. Belitz and T. R. Kirkpatrick, Rev. Mod. Phys. **66**, 261 (1994).
- ⁶ A. M. Finkelshtein, Sov. Phys. JEPT **75**, 97 (1983); C. Castellani, C. DiCastro, P.A. Lee, and M. Ma, Phys. Rev. B **30**, 527 (1984); M. A. Tusch and D. E. Logan, Phys. Rev. B **48**, 14843 (1993); *ibid.* **51**, 11940 (1995); D. L. Shepelyansky, Phys. Rev. Lett. **73**, 2607 (1994); P. J. H. Denteneer, R. T. Scalettar, and N. Trivedi, Phys. Rev. Lett. **87**, 146401 (2001).
- ⁷ K. Byczuk, W. Hofstetter, and D. Vollhardt, cond-mat/0403765.
- ⁸ J. Hubbard, Proc. Roy. Soc. London **281**, 401 (1964).
- ⁹ H. von Dreifus and A. Klein, Commun. Math. Phys. **124**, 285 (1989).
- ¹⁰ A. D. Mirlin and Y. V. Fyodorov, Phys. Rev. Lett. **72**, 526 (1994); J. Phys. I France **4**, 655 (1994); M. Janssen, Phys. Rep. **295**, 1 (1998) and references therein.
- ¹¹ D. Lloyd, J. Phys. C**2**, 1717 (1969); D. Thouless, Phys. Reports **13**, 93 (1974); F. Wegner, Z. Phys. B **44**, 9 (1981).
- ¹² The most probable value of a random quantity is defined as that value for which its probability distribution function becomes maximal.
- ¹³ *Log-normal distribution-theory and applications*, ed. E. L. Crow and K. Shimizu (Marcel Dekker, inc. 1988).
- ¹⁴ E. W. Montroll and M. F. Schlesinger, J. Stat. Phys. **32**, 209 (1983); M. Romeo, V. Da Costa, and F. Bardou, Eur. Phys. J. B **32**, 513 (2003).
- ¹⁵ V. Dobrosavljević and G. Kotliar, Phys. Rev. Lett. **78**, 3943 (1997).
- ¹⁶ V. Dobrosavljević, A. A. Pastor, and B. K. Nikolić, Europhys. Lett. **62**, 76 (2003).
- ¹⁷ G. Schubert, A. Weiße, and H. Fehske, cond-mat/0309015.
- ¹⁸ W. Metzner and D. Vollhardt, Phys. Rev. Lett. **62**, 324 (1989).
- ¹⁹ A. Georges, G. Kotliar, W. Krauth, and M.J. Rozenberg, Rev. Mod. Phys. **68**, 13 (1996).
- ²⁰ Th. Pruschke, M. Jarrell, and J. K. Freericks, Adv. in Phys. **44**, 187 (1995).
- ²¹ D. Vollhardt, *Correlated Electron Systems*, vol. 9, ed. V. J. Emery, (World-Scientific, Singapore, 1993), p. 57.
- ²² V. Janiš and D. Vollhardt, Phys. Rev. B **46**, 15712 (1992); M. Ulmke, V. Janiš, and D. Vollhardt, Phys. Rev. B **51**, 10411 (1995).
- ²³ R. Vlaming and D. Vollhardt, Phys. Rev. B **45**, 4637 (1992).
- ²⁴ F. X. Bronold, A. Alvermann, and H. Fehske, Phil. Mag. **84**, 637 (2004).
- ²⁵ L.M. Falicov and J.C. Kimball, Phys. Rev. Lett. **22**, 997 (1969).
- ²⁶ J.K. Freericks and V. Zlatić, Rev. Mod. Phys. **75**, 1333-1382 (2003) and references therein.
- ²⁷ P.G.J. van Dongen and C. Leinung, Ann. Phys. **6**, 45 (1997).
- ²⁸ J.K. Freericks and R. Lemański, Phys. Rev. B **61**, 13438 (2000).
- ²⁹ D. O. Demchenko, A. V. Joura, and J.K. Freericks, Phys. Rev. Lett. **92**, 216401 (2004).
- ³⁰ U. Brand and C. Mielsch, Z. Phys. B **75**, 365 (1989).
- ³¹ D.N. Zubarev, Sov. Phys. Usp. **3**, 320 (1960).
- ³² R. Bulla, A. C. Hewson, and Th. Pruschke, J. Phys.: Condens. Matter **10**, 8365 (1998).
- ³³ For a uniform probability distribution function and N discrete values of $A(\omega, \epsilon_i)$ one finds $A_{\text{geom}}(\omega) = \left(\prod_{i=1}^N A(\omega, \epsilon_i)\right)^{1/N} = \exp\{[\sum_{i=1}^N \ln A(\omega, \epsilon_i)]/N\}$. Hence $A_{\text{geom}}(\omega)$ vanishes if any of the $A(\omega, \epsilon_i)$ is zero. The arithmetic average does not have such a property.
- ³⁴ C.M. Soukoulis and E.N. Economou, Waves Random Media **9**, 255 (1999).
- ³⁵ Q. Si, G. Kotliar, and A. Georges, Phys. Rev. B **46**, R1261 (1992).
- ³⁶ F. Gebhard, *The Mott Metal-Insulator Transition*, Springer Tracts in Modern Physics 137 (Springer-Verlag Berlin Heidelberg New York, 1997), p. 217.
- ³⁷ R. Bulla and M. Potthoff, Eur. Phys. J. B **13**, 257 (2000).
- ³⁸ e.g. R. Lemański, cond-mat/0410245.
- ³⁹ E. Dagotto, T. Hotta, and A. Moreo, Phys. Rep. **344**, 1 (2001).
- ⁴⁰ I. Zutic, J. Fabian, and S. Das Sarma, Rev. Mod. Phys. **76**, 323-410 (2004).
- ⁴¹ T. Dietl, Semicond. Sci. Technol. **17**, 377 (2002).

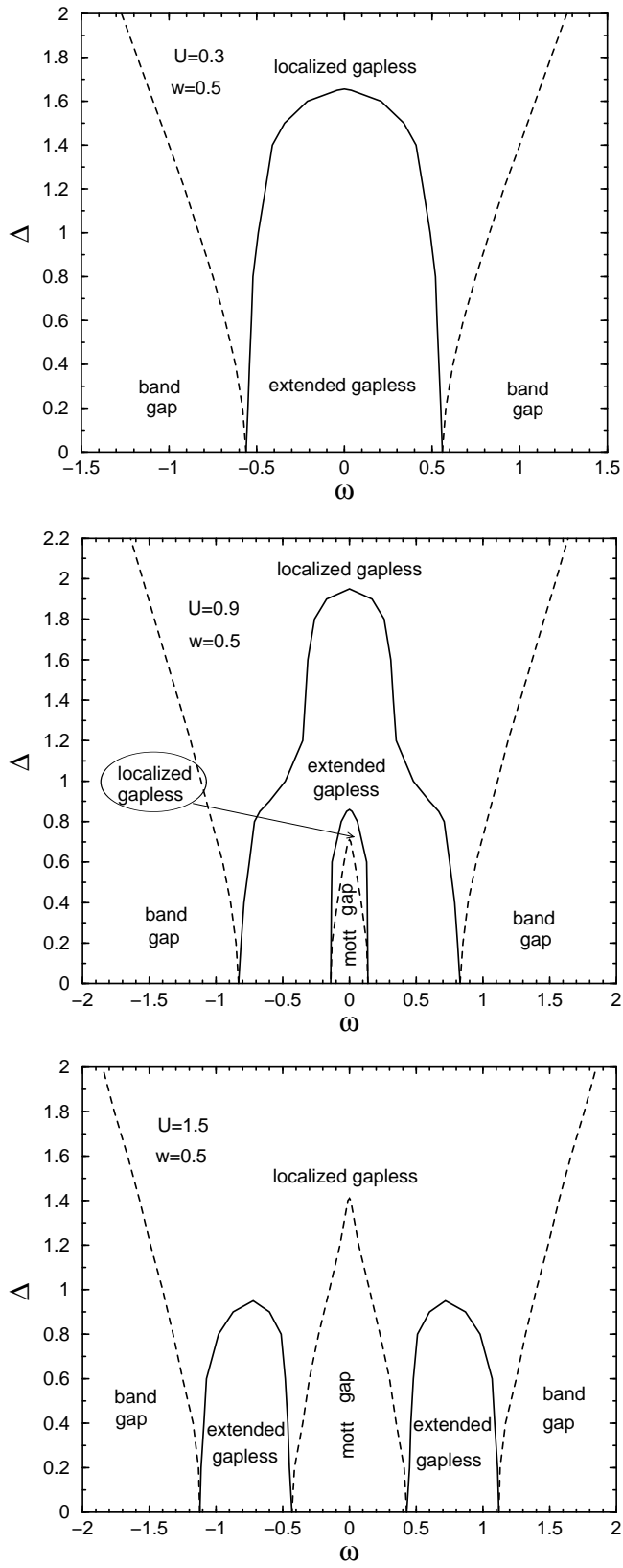


FIG. 1: Spectral phase diagrams of the ground states without a long-range orders for the Anderson-Falicov-Kimball model with $w = 0.5$ at $U = 0.3$ (upper panel), $U = 0.9$ (middle panel), and $U = 1.5$ (lower panel). Solid lines show mobility edges determined within DMFT with geometric averaging and dashed lines present band edges determined within DMFT with arithmetic averaging.

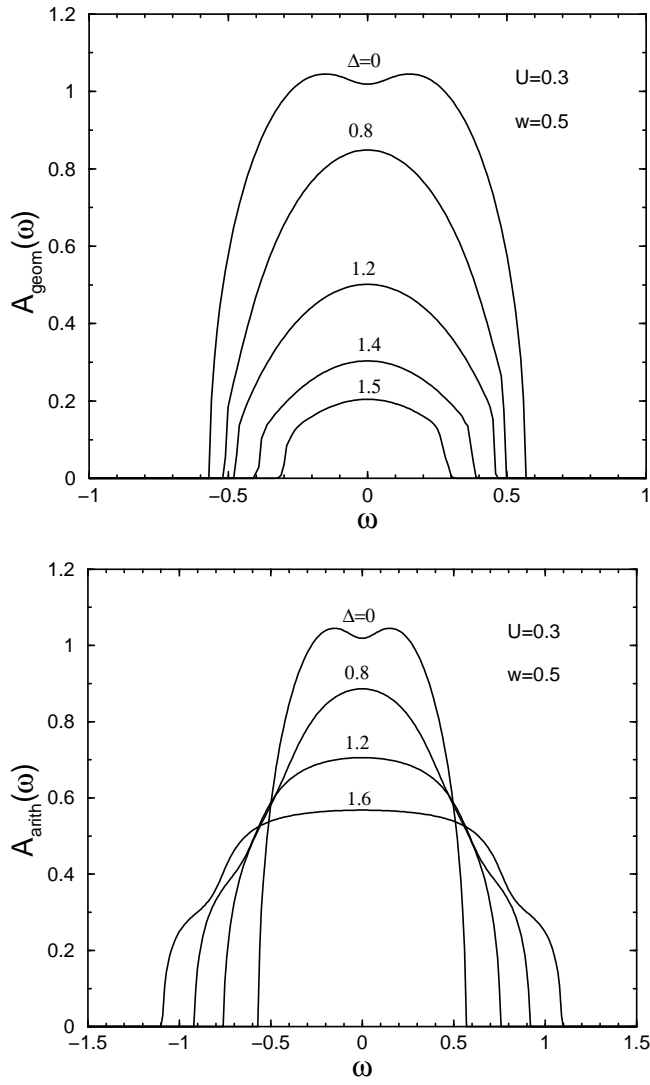


FIG. 2: Geometrically (upper panel) and arithmetically (lower panel) averaged local density of states at $w = 0.5$ and $U = 0.3$ for different disorder strength Δ . Vanishing of A_{geom} upon increasing Δ is a signature of the Anderson localization.

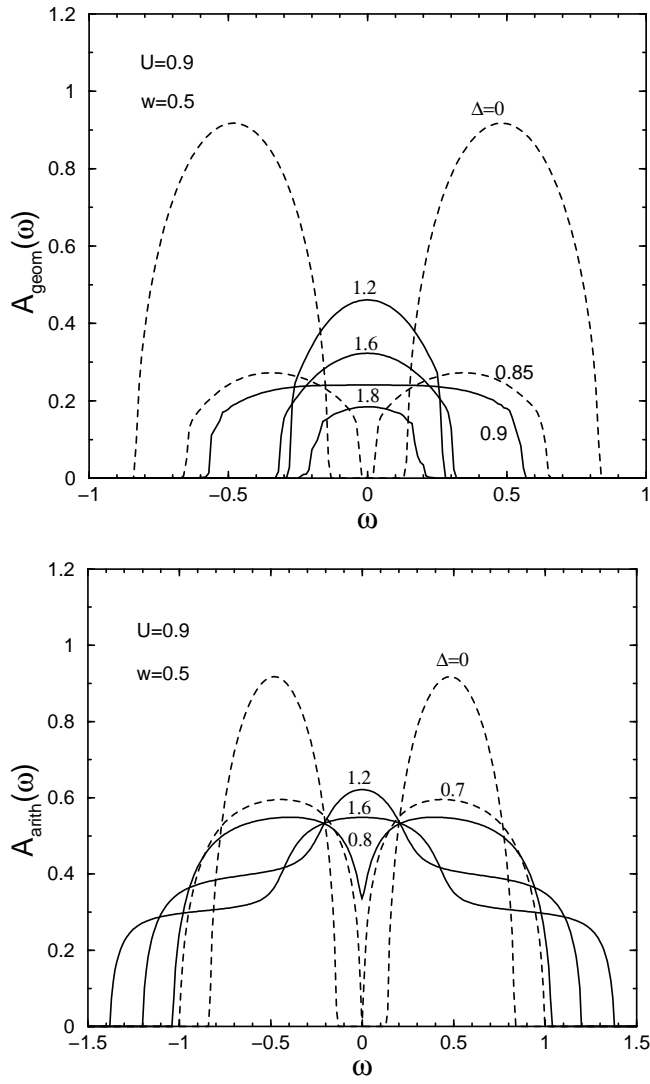


FIG. 3: The same as in Fig. 2 but at $U = 0.9$. The correlation (Mott) gap is closed by strong disorder and the system becomes a bad metal.

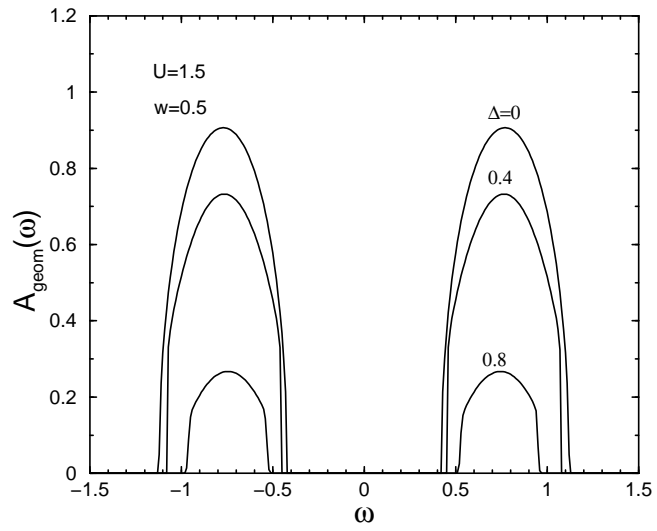


FIG. 4: Geometrically averaged local density of states at $w = 0.5$ and $U = 1.5$ for different disorder strength Δ .

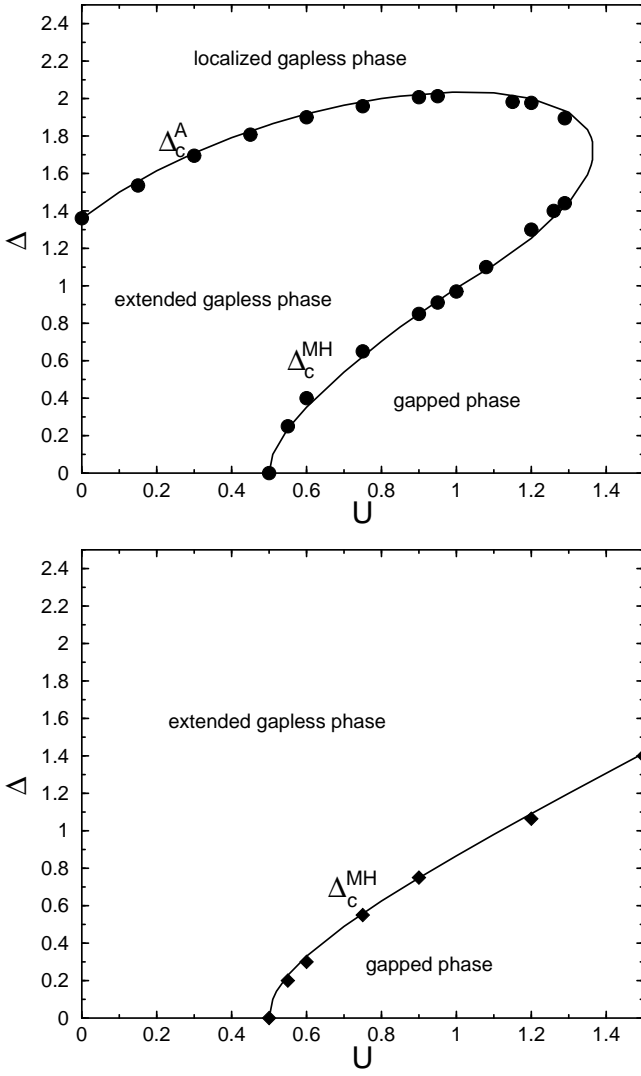


FIG. 5: Ground state phase diagrams for particles in a band center determined by using geometric (upper panel) and arithmetic (lower panel) means. Dots and squares are determined from the numerical solution of the DMFT equations. Solid lines are obtained analytically from the linearized DMFT.

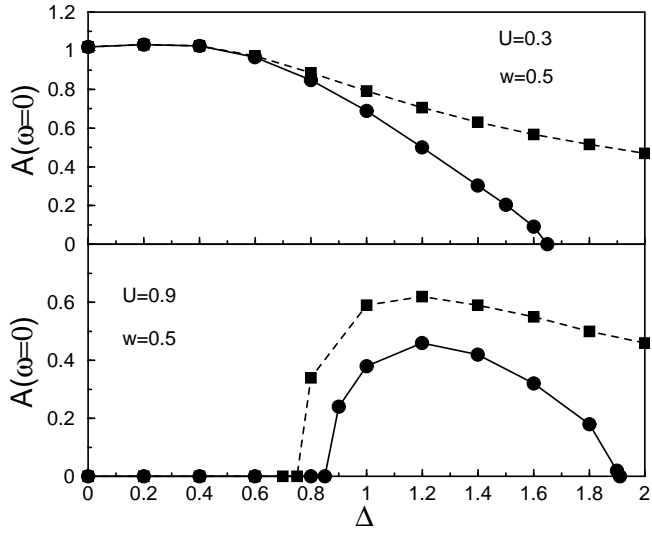


FIG. 6: Local density of states in a band center ($\omega = 0$) as a function of disorder Δ at $w = 0.5$ with $U = 0.3$ (upper panel) and $U = 0.9$ (lower panel). Solid (dashed) lines are determined by using geometric (arithmetic) averaging.

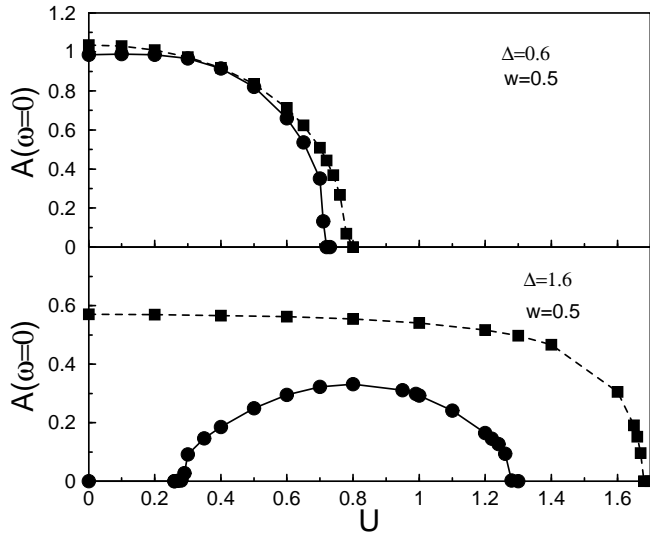


FIG. 7: Local density of states in a band center ($\omega = 0$) as a function of interaction U at $w = 0.5$ with $\Delta = 0.6$ (upper panel) and $\Delta = 1.6$ (lower panel). Solid (dashed) lines are determined by using geometric (arithmetic) averaging.